Pol. J. Environ. Stud. Vol. 31, No. 4 (2022), 3249-3261
DOI: *10.15244/pjoes/145607* ONLINE PUBLICATION DATE: 2022-04-07

Original Research

Flood Susceptibility Assessment Using Frequency Ratio Modelling Approach in Northern Sindh and Southern Punjab, Pakistan

Awais Munir[1], Muhammad Asad Ghufran[1], Syeda Maria Ali[1], Asma Majeed[2]*, Aniqa Batool[3], Muhammad Bachal Alias Sahib Khan[2], Ghulam Hassan Abbasi[2]

[1]Department of Environmental Science, International Islamic University Islamabad, Pakistan
[2]Department of Environmental Science, The Islamia University of Bahawalpur, Pakistan
[3]Department of Environmental Sciences, PMAS Arid Agriculture University, Rawalpindi, Pakistan

Received: 17 September 2021
Accepted: 7 January 2022

Abstract

Flooding is among the most catastrophic and common natural events. It not only endangers human lives, their livelihoods, and possessions but also devastates the nation's economy. Increased flooding is an inevitable consequence of climate change. Hence, Identification of flood suspectable hotspots is vital for flood risk management along with disaster handling. The primary objective of this research is to use a frequency ratio model to classify flood-prone zones in two provinces of Pakistan. The flood inventory map was developed using 230 flood location points in Northern Sindh and Southern Punjab. Aspect, profile curvature, elevation, slope, normalized difference vegetation index (NDVI), normalized difference soil index (NDSI), distance from the road, distance from the river, land use/land cover (LULC) and rainfall were among the ten (10) determining factors. The data were randomly divided into two distinct datasets, with 70% flood points (161) used for inventory formulation and the other 30% (69 flood points) for result validation. The flood vulnerability map was categorized into five different zones ranging from very low (19.73%) to very high (20.37%) susceptibility range. The area under the receiver operating characteristic curve (ROC) and area under curve (AUC) was used to demonstrate the prediction result that yielded a reasonable score of 77.4%. The study suggested that in comparison to other studied districts, Jacobabad is the most prone region with acute vulnerability and constrained resilience. The presented data can serve as a source for tracking, assessing, and predicting potential flood activity in the area and could be beneficial for planners and decision-makers involved in early disaster response planning within the country.

Keywords: flood susceptibility, GIS modelling, flood inventory mapping, conditioning factors, frequency ratio modelling

*e-mail: asmamajeedrana@gmail.com

Introduction

Every year, various natural disasters such as earthquakes, floods, drought, and landslides cause a large number of deaths and property damage around the world [1]. Among all other disasters, flooding is one of the most destructive natural disasters that occur when a large amount of water exceeds its usual limits, inundating river banks and causing water retention for a short period [2]. Floods are a major factor destroying the environment, transportation systems, agriculture, sociocultural and human life accounting for almost 40% of all-natural disaster losses [3-5]. The size of the flood is one of the most significant aspects while increased harm has been attributed to urbanization and population growth along rivers and decline in forest areas. Poor infrastructure, social mentality, low resilience, and deficiency of long-term mitigation steps are also among important determining factors [6, 7]. Almost one-third of the world's land area is vulnerable to the risk of flooding [8]. Flood-related damages caused 32% of human and environmental harm between 1963 and 1992 and affected an average of 99 million people from 2000 to 2008 [9]. China is the most affected country, in terms of facing the social and economic effects of flooding [10, 11] Failure of the dam as a result of the heavy rains has also triggered floods in downstream areas. In 1979, the collapse of the Machu dam in marvi, Saurashtra, resulted in immense losses of land, crops, livestock, and approximately 10,000 human live [12]. Unless appropriate flood prevention measures are taken, the number of people vulnerable to catastrophic flooding will continue to increase [13].

Between 2000 and 2013, Pakistan was hit by 25 natural disasters, the most prevalent of which were floods, earthquakes, and landslides [14]. Floods were particularly severe in 1942, 1956, 1957, 1958, 1973, 1975, 1976, 1979, 1992, 1994, 1995, 2003, 2005, 2007, 2010, 2011, and 2013. One of the worst floods in Pakistan's history hit in August 2010, while between 1947 and 2010 approximately 8000 people died and approximately $10 billion was lost in economic losses [15]. Summer floods in Pakistan are mostly caused by monsoon rainfall. The historical 2010-11 floods in the study region were the worst in terms of severe and extended rainfall, large flood discharge, the number of people impacted and their property destruction [16]. Abnormal rainfall was recorded by almost all the metrological stations in the country and the main cause behind this disastrous flooding was the consecutive rainfall for four days (27-30 July) [17]. During 2010, 2011, and 2013 years, there have been riverine floods in Northern Sindh and Southern Punjab areas. The Districts of Northern Sindh, Jacobabad, Larkana, and Sukkur were badly affected. Similarly, in summer 2010, unusually heavy rain and river breaches in the Sothern Punjab's District Rahimyar Khan and Bahawalpur caused an unprecedented riverine flood. Structures were destroyed, irrigation channels and linking roads were damaged, crops and orchards were washed away [18].

Flooding is a devastating natural hazard that is almost impossible to fully eradicate, modeling flood susceptibility is one of the latest strategies used for dealing with flood disasters. Remote sensing and GIS software techniques have become increasingly popular in recent decades because they add a whole new dimension to risk assessment and justification. Satellite image analysis on the RS and GIS platforms yielded adequate results for flood susceptibility and vulnerability mappings as it provides an incredible environment to run and manipulate a wide range of models to assess flood vulnerability with rational and reliable results [19]. It is critical to develop flood susceptibility mapping and flood risk assessments as it can enable government officials and planners to develop appropriate flood control plans and propose management schemes for reducing flood vandalism in the future [20].

Study Area

(Fig. 1) Punjab's climate is vulnerable, because of its geographical position, low adaptability, and a high reliance on the natural surroundings. This province has an estimated population of 93 million people.

Sindh is Pakistan's most heavily inhabited and urbanized province, accounting for 24% of the country's overall population. Sindh's population grew from 41.248 million people in 2010 to 45.998 million people in 2015 [21]. Due to monsoon and the Indus River, Northern Sindh and Southern Punjab's floodplain are susceptible to recurrent flooding during the summer season. Because it flows along a ridge, the Indus River in Northern Sindh and Southern Punjab is treacherous. It is known for its ability to change course and the outflowing water once breached cannot be discharged back into the river [15]. A considerable number of villages are existent next to the river catchment and population settlements are encroaching toward risky locations in the study area [22]. Historical data indicate that three extreme and fourteen moderate riverine and flash flood incidences occurred between 1942 and 2013 in Pakistan's northern Sindh and Southern Punjab region, which destroyed natural resources and thousands of lives [23]. There is a lack of flood susceptibility assessment and mapping. To emphasize this problem, attempts were made to research certain factors to better identify and forecast areas that are more vulnerable to flooding. This study was conducted to find out the future susceptibility of flood disasters in the chosen study areas that include Bahawalpur and Rahim yar Khan in southern Punjab and Sukkur, Larkana and Jacobabad in Northern Sindh. The main goal of the study is to examine flood-prone areas and the usage of frequency ratio (FR) model to create flood vulnerability map for selected regions. The FR model is a GIS-based method that is known to generate scientifically valid

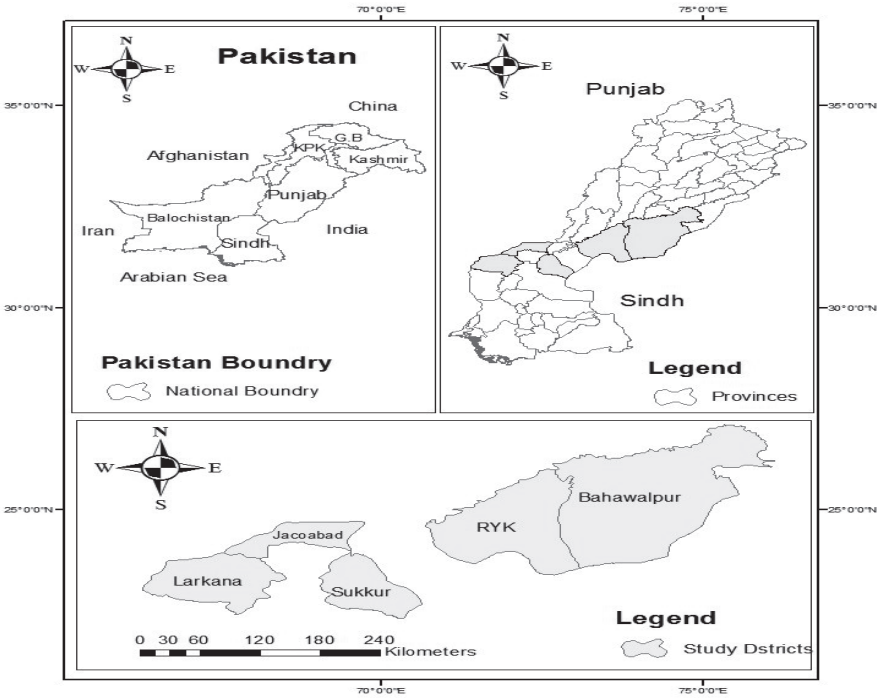

Fig. 1. Map of the study area.

flood susceptibility maps [24]. Flood risk modeling is crucial for its management [25]. It involves various relevant factors such as drainage, density, slope, land use, elevation, rainfall deviation, lithology, and land use/cover. All these factors can be used with the help of the FR model to identify very high to very low susceptibility zones. These findings will be useful to planners, researchers, and local governments for impact assessments to predict future potential flood zones and activity in the area and could be beneficial for planners and decision-makers involved in early disaster response planning within the country.

Experimental

Materials and Methods

The flood susceptibility modelling involves a number of steps. The presented flow chart demonstrates the summary of the followed methodology that consist of four main steps including spatial database preparation, flood inventory mapping, origination of flood conditioning factors and bivariate statistical analysis of the flood conditioning factors using frequency ratio modeling.

Spatial Database Preparation

The spatial database preparation is a significant step in the flood vulnerability and susceptibility analysis process, as it entails the collection of appropriate factors of floods [26]. Floods cannot be caused by a single factor in most cases. Many parameters like climate and geomorphologic composition regularize the occasion of floods and their intensity [27]. The multi-criteria analysis MCA-based flood susceptibility and susceptibility assessment will be more reliable and authenticate instead of single criteria-based flood susceptibly analysis [28, 29]. (Table 1) (Fig. 2).

Flood Inventory Map

The precision with which flood events are recorded has a huge effect on the mapping of flood vulnerability and susceptibility [30]. A total of 230 location points for flood were chosen for the inventory. Since using the polygon layout of the catalog is challenging for the algorithm and results amplification, random points were used in the study. This format for Inventory data has been used in the majority of related natural hazard modeling [31]. For training and testing, the map was divided into 70% -30% ratios [32]. Training locations (161 points) were chosen at random for the generation of the dependent results, which consisted of 0 and 1 values, with 1 indicating the presence of flooding and 0 indicating the nonexistence of flooding. As a non-flooding point, equivalents of 69 points were selected. (Fig. 3).

Flood Conditioning Factors

It is very critical to identify the important factors that influence flood occurrence in establishing flood susceptibility maps [33]. As a result, in flood susceptibility modeling ten (10) conditioning factors

Table 1. Flood predicting factors and their cell size.

Parameters	Sub-classification	Resolution
Flood record area's	Flood extent	Point coordinates
	Elevation (m)	30 m
	Slope angle (Degree)	30 m
	Aspect	30 m
	Profile curvature	30 m
Flood predicting factors	Distance from road (m)	30 m
	Distance from river (m)	30 m
	NDSI	30 m
	NDVI	30 m
	Mean annual rainfall (mm)	30 m

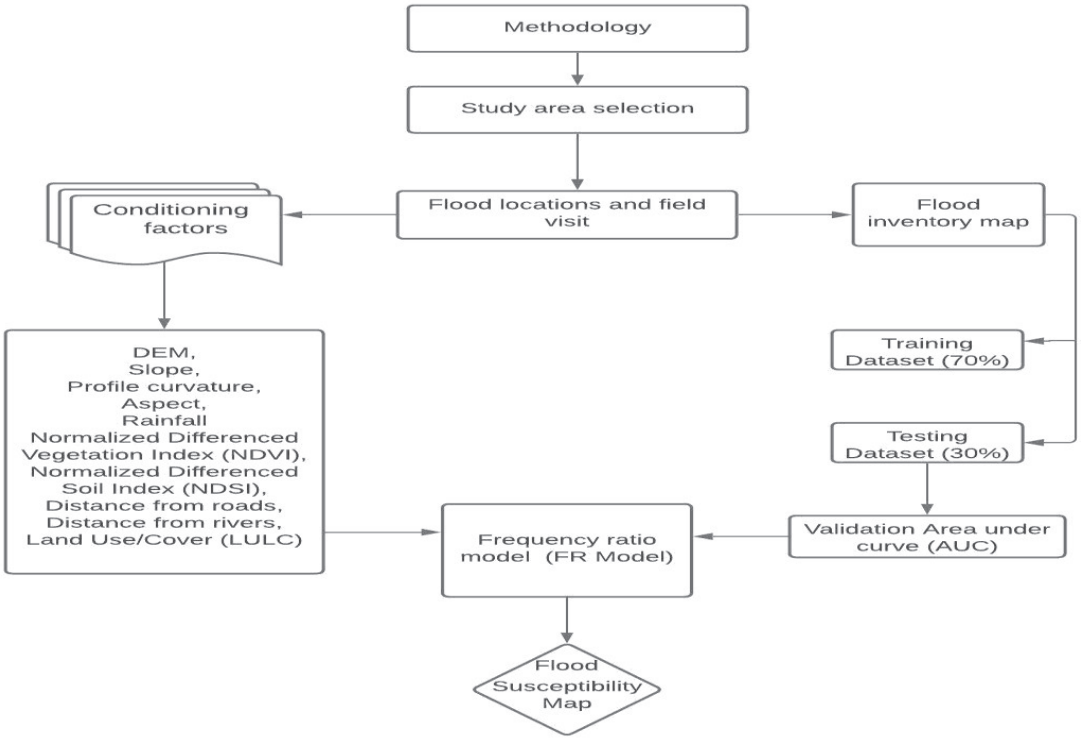

Fig. 2. Flow chart of the methodology for preparing flood susceptibility map.

with 30* 30-mpixel size were used: (1) Aspect, (2) Slope, (3) Elevation, (4) Profile Curvature, (5) Normalized Difference Soil Index (NDSI), (6) Normalized Difference Vegetation Index (NDVI), (7) Distance from the river, (8) Distance from the road, (9) Land use land cover map (LULC), and (10) Rainfall. It's essential to note that topographic data has a significant effect on modeling results and that a lot of research is limited by a lack of accurate topographic data [34]. Derivative factors and topography play a significant role in determining flood susceptibility and vulnerability [35].

(Fig. 4) Previous 29 years' data of mean annual rainfall (1989-2018) was taken from the Pakistan metrological Department (PMD). Digital elevation model (DEM) is one of the most useful techniques for flood prediction which provides a three-dimensional view of the ground surface terrain. The DEM for the study districts was obtained by the Shuttle Radar Topography Mission SRTM with a resolution of 30 m obtained from Earth Atmosphere and NASA (http://www.dwtkns.com/srtm30m). The Euclidean distance tool of the Spatial Analyst tool in ArcMap 10.2 was used to establish the layers of distance from rivers and distance from roads. The profile curvature (Fig. 4d) was used in this analysis because it influences the flow rate of water draining the soil. ArcMap measured it using

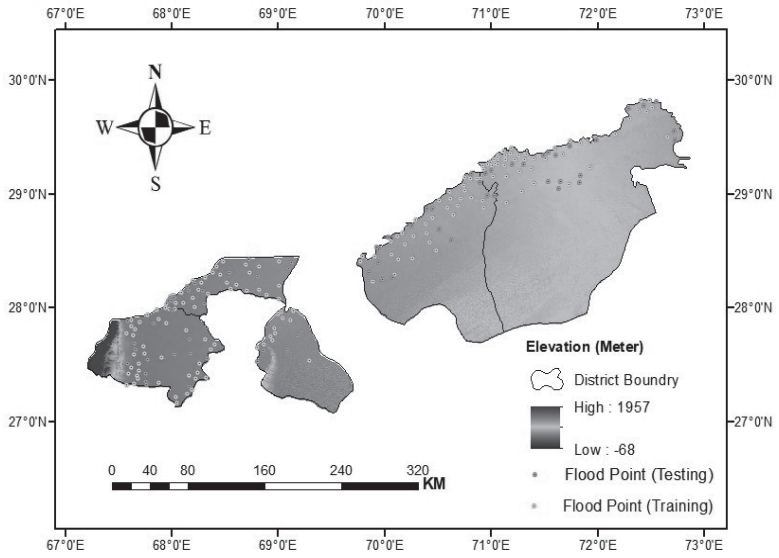

Fig. 3. Flood inventory map of the study area.

the spatial analyst tool. The vegetation and soil are also essential factors in determining flood susceptibility [34]. The Normalized Difference Vegetation Index (NDVI) and the Normalized Difference Soil Index (NDSI) were calculated and gained by using different bands from Landsat 8 OLI satellite images assembled by the USGS EROS data center by using diverse bands from Landsat 8 OLI satellite images. NDSI Fig. 4f) is an analytical method for improving soil data from vegetation and impermeable surfaces. It was calculated using the band ratio method in ArcGIS (Raster calculator) to distinguish soil from other ground cover forms to a degree, with high values indicating exposed soil areas and low values indicating other categories which also include vegetated areas [36]. NDVI Fig. 4e) was also determined to illustrate the differences in vegetation's spectral responses in the red plus near-infrared bands low values contribute to bare areas of rock/sand or snow and high values suggest temperate rainforests and tropical rainforests. Equations (1) and (2) were then used to calculate respectively.

$$NDSI = \frac{\text{Band7}-\text{Band3}}{\text{Band7}+\text{Band3}} \quad (1)$$

$$NDVI = \frac{\text{Band5}-\text{Band4}}{\text{Band5}+\text{Band4}} \quad (2)$$

Frequency Ratio Model

It is very critical to differentiate the conditioning factors and conditions which can trigger flooding when determining the probability of flooding over a specific period in a particular environment [37]. For flood susceptibility mapping, there are several models and techniques from which to choose. The frequency ratio model [38] is a highly suitable technique for hazards identification amid a high exactness rate. The frequency ratio (FR) is a method of bivariate statistical analysis (BSA), in which each class of a parameter is assigned a value, and its effect on flood occurrence is assessed [39]. The FR approach was used in conjunction with GIS techniques to conduct the study of flood vulnerability and susceptibility. For BSA, FR is a very reliable method since it considers the effect of every conditioning factor on flooding and assigns weights very accurately. The FR method is determined by the relationship b/w flooding spread and every conditioning factor, and it is used to show the relationship between flood locations and floods conditioning factors in the research study field. If the FR value is greater than 1, the percentage of flooding is greater than the region, indicating a stronger correlation; however, values less than 1 indicate a weaker correlation [40]. The evaluation of flood susceptibility mapping is critical for identifying flood-related factors. Historical flooding events and their triggering parameters may be used to derive the relationship between flood and linked conditioning factors that can cause flooding [41]. The assessment of flood susceptibility mapping is critical for identifying flood-related factors. Historical flooding events and their triggering parameters may be used to derive the relationship between floods and linked conditioning factors that can cause flooding. The Flood Frequency Ratio (FR) is determined by looking at the relationship b/w flood events and the factors that provide the reasons. As a result, the FR of each class of each conditioning factor was determined concerning earlier flood occurrence as shown in Table 2. Frequency Ratio (FR) values were obtained and calculated by via following given formula (3):

$$FR = \left[N_{pix}(SX_i)/\sum_{i=1}^{m} SXi\right]/\left[N_{pix}(Xj)/\sum_{j=1}^{n} N_{pix}\,(Xj)\right] \quad (3)$$

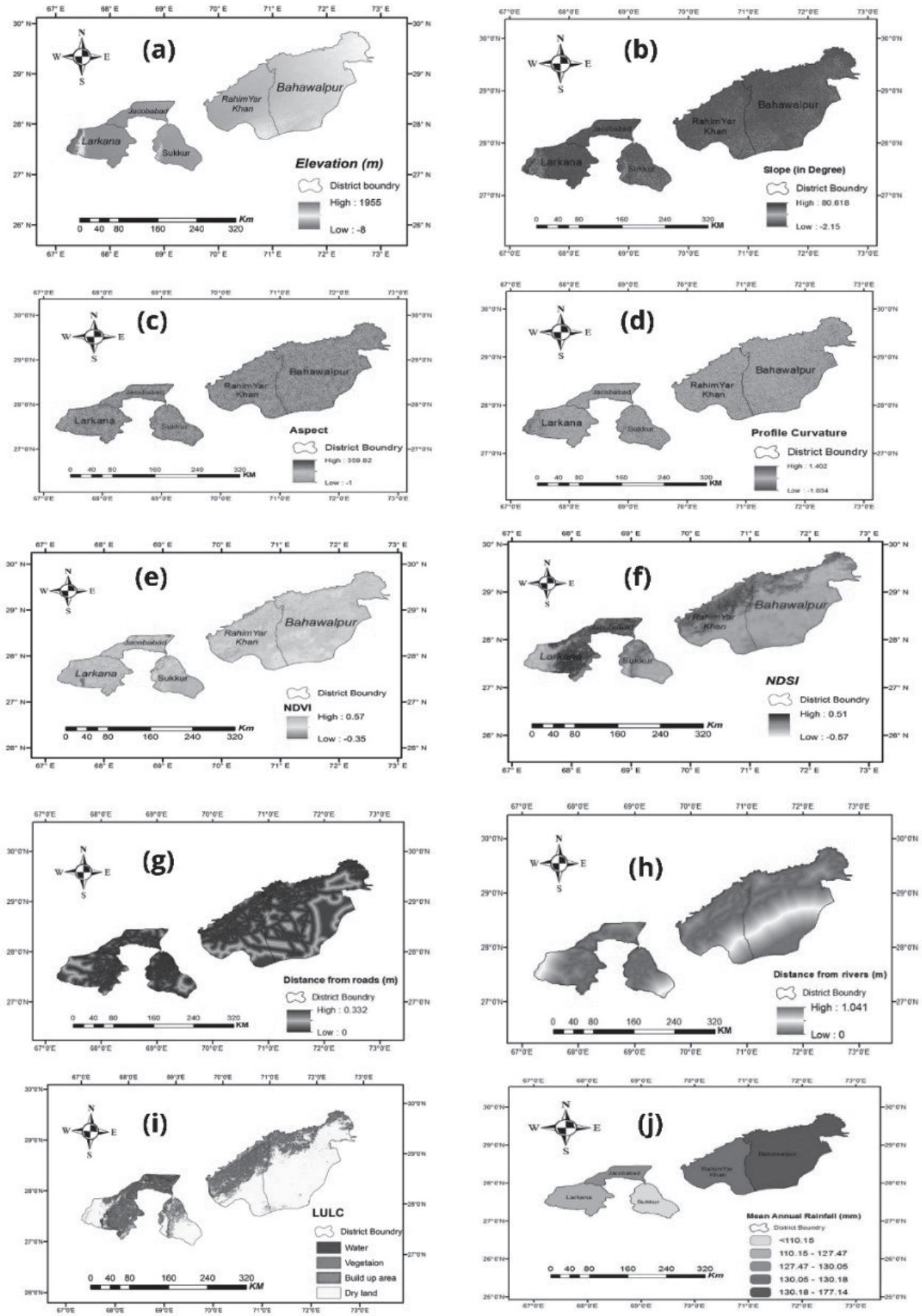

Fig. 4. Predicting factors of flood susceptibility map: a) Elevation, b) Slope, c) Aspect, d) Profile curvature, e) NDVI, f) NDSI, g) Distance from road, h) Distance from road, i) LULC, j) Mean annual rainfall.

After calculating the Frequency Ratio values for each class, every controlling factor added all of the values together to generate the final flood vulnerability or susceptibility map. The flood risk map formula is given:

In the next step, the FR is normalized as the relative frequency (RF) for a range of probability levels [0, 1] using equation (4).

$$RF = \frac{Factor\ class\ FR}{\sum Factor\ class\ FR} \quad (4)$$

After normalization, the RF also has the downside of assigning equal weight to all causative variables. To solve this trouble and discover the mutual interdependence of flood contributory factors, a (PR) predictor rate or weight was determined by ranking each flood contributory factor using the training data set equation (5).

$$PR = (RF_{max} - RF_{min})/(RF_{max} - RF_{min}) \quad (5)$$

Table 2. Calculation results of FR and RF for all classes of factors.

Factors	Factor classes	No of points	% of points	Class area	% of class area	FR	RF
Elevation	1	6220113	86.81	300.41835	98.5	2.5	0.69
	2	443751	6.19	2.143223	0.7	8.57	0.23
	3	2591941	3.61	1.251596	0.4	1.82	0.05
	4	174696	2.43	0.843745	0.3	2.47	0
	5	66895	0.93	0.323089	0.1	2.57	0
Slope	1	10608913	13.6	0.092251	21.8	9.7	0.31
	2	15176643	19.46	0.103423	24.44	7.57	0.24
	3	20461498	26.24	0.115555	27.3	6.25	0.19
	4	16284928	20.88	0.069604	16.45	4.72	0.15
	5	15425436	19.78	0.042273	9.99	3.04	0.09
Aspect	1	12219715	19.35	0.098066	23.13	8.92	0.23
	2	10909733	17.27	0.067587	15.97	6.87	0.18
	3	14383836	22.77	0.091703	21.67	7.09	0.19
	4	13095650	20.73	0.084868	20.05	7.17	0.19
	5	12536681	19.85	0.080866	19.11	7.17	0.19
Curvature	1	1342501	2.12	0.007027	1.66	5.95	0.17
	2	3602535	5.7	0.019407	4.58	6.1	0.17
	3	21251814	33.65	0.14286	33.76	7.48	0.21
	4	20372308	32.26	0.154652	36.55	8.44	0.24
	5	16576458	26.25	0.099145	23.43	6.63	0.19
NDVI	1	11404628	23.81	733.404549	1.37	0.13	0.37
	2	11391449	23.79	23878.19214	44.9	0.07	0.22
	3	12722976	26.57	12904.39117	24.26	0.02	0.08
	4	12362658	25.81	7975.387359	14.99	0.02	0.06
	5	11197031	23.38	7669.423643	14.44	0.08	0.25
NDSI	1	11426523	19.34	10283.85754	19.34	0.01	0.05
	2	13079095	22.13	11771.17044	22.13	0.01	0.05
	3	12640331	21.39	11376.28334	21.39	0.04	0.12
	4	10862412	18.38	9776.15829	18.38	0.08	0.25
	5	11070380	18.73	9953.32925	18.73	0.18	0.52

Table 2. Continued.

Distance from river	1	13789599	21.83	0.13027	30.79	1.05	0.35
	2	17358181	27.48	0.170938	40.4	1.09	0.36
	3	16254768	25.74	0.119756	28.3	8.18	0.27
	4	15743067	24.93	0.002127	0.5	1.27	0
Distance from road	1	1	0	0.068071	16.08	0	0.99
	2	15338998	24.29	0.103985	24.57	7.56	9.95
	3	16466134	26.07	0.12176	28.77	8.19	1.07
	4	16045568	25.41	0.105401	24.91	7.29	9.59
	5	15294914	24.22	0.023873	5.64	1.76	2.32
LULC	1	12730113	21.24	96.91525914	21.54	0.18	1
	2	11622270	19.67	2.835608358	19.67	0.09	0.29
	3	18839280	31.88	2.135449098	31.88	0.01	0.05
	4	10552058	17.86	60.75866314	17.86	0	0.03
	5	5335021	9.03	33.38357293	9.03	0.02	0.07
Rainfall	1	4065	10.09	0.044286	10.45	1.2	0.1
	2	5478	13.6	0.173151	40.87	3.5	0.31
	3	2727	6.77	0.143627	33.9	5.86	0.52
	4	9529	23.66	0.051909	12.25	6.08	0
	5	18470	45.86	0.010648	2.51	6.49	0

Lastly, the flood susceptibility index was calculated by summing the PR of each factor and the RF of each class using equation (6).

$$FVI = \sum_{j=1}^{n} FR \tag{6}$$

where $N_{pix}(SX_i)$ is the number of flood points in class I of variable X, $N_{pix}(X_j)$ is the integral of pixels in variable X_j, m is the total classes in the variable X_i, total factors of the study region are the n [35].

Model Validation

It is important to categorize areas that could be affected by potential flooding while conducting a flood susceptibility study. To validate the susceptibility maps is very important concerning known potential floods, despite the validation method used [42]. The region beneath the curve is a common, all-encompassing technique of assessing accurateness that can be used to assess forecast and success rates [43]. The justification or validation method was carried out by comparing defined flood data with the likelihood map of acquired flooding, using AUC [44]. This gave a strong classification with AUC = 1 and a random classification with AUC = 0.5. AUC has been used in a variety of experiments to assess the efficacy of susceptibility mapping [45]. The techniques include splitting the probability map into equal-area categories, with the performance and prediction curves determining each probability category. On the x-axis, percentages of flood-prone areas are plotted from maximum to minimum, and percentages of % of flood actions are plotted on the y-axis. A steeper curve suggests that a larger proportion of flood actions or events fall into more susceptible categories.

Results and Discussion

Several independent variables, referred to as factors for ideal conditions, play a precise role in flood susceptibility and vulnerability mapping [43]. All ten conditioning variables, including elevation, NDVI, NDSI, slope, aspect, curvature, distance from the path, Distance from the river, LULC, and rainfall, each have their spatial distribution and statistical database. The elevation is a significant factor in flood incidence as water often flows from higher locations to lower land areas [46]. Previous research has found a low likelihood of flooding in higher elevation areas and a high likelihood of flooding in the lowland areas [47]. Generally, the Frequency Ratio value will decline as the height of the area increases [48]. Table 2 shows the 2 lower elevated classes in the study region (183 m and 183 to 442 m) have high-Frequency Ratio values of

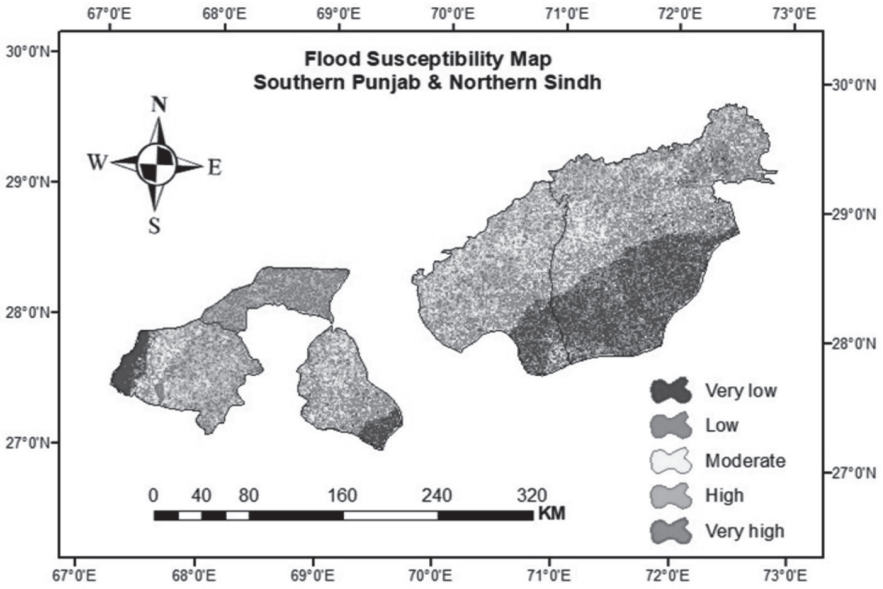

Fig. 5. Flood susceptibility map using FR model.

2.5 & 8.5, respectively, indicating a high likelihood of flooding in low elevated areas. Flooding is less probable in areas with a low FR value and a high altitude [59].

Slope controls the occurrence of flooding, so low-level land areas in rainy spells have a close link to the flood situation. Flooding and flood events are more likely to occur when the slope gradient is lower [50]. The infiltration method is often influenced by the gradient of the slope. An increasing gradient reduces penetration but surface runoff increases; so the result, in areas with abrupt descent gradient, a large amount of water becomes inactive, resulting in flooding [51]. The findings show that the two lower slope gradient grades, <2.39° and 2.39°-5.31°, respectively, have the maximum FR values of 9.7 and 5.7. The slope gradient above 24.7°, the other side shows the lowest FR value of 3.04. 2) Table. Approximately 59.3% of strong floods occurred in study areas with a slope of less than 12.1%. Since the aspect is linked to physiographic trends and soil moisture patterns, it can be useful in hydrologic situations [52]. Aspect has a significant impact on hydrologic processes such as evapotranspiration and frontal precipitation direction, as well as weathering and vegetation growth, particularly in drier climates [53]. In this study area, the results showed that ranges between 65 and 283 to 359 had high FR values of 8.9 and 7.1. Curvature is also a significant element that reflects the topography's morphology [54]. There are three different types of curvature maps. A convex surface has a positive curvature value, a flat and plane surface has a zero-curve value, and a concave surface has a negative curvature value [47]. The results show that the flat surface had the highest RF of 0.61, while the concave surface had the lowest RF of 0.15. (Table 2). It was revealed that approximately 83 percent of previous floods occurred on slopes with a flat or convex form. The NDVI is another significant flooding conditioning element. The index's range values are from -1 to +1 [49]. According to Khosravi, an indication of water is shown by negative values and positive (+ve) values indicate vegetation, thus NDVI has a negative (-ve) association with flooding. Higher NDVI values suggest a lower or lesser flood risk, while lower NDVI values indicate a higher flood risk [55]. The NDVI values in this sample range from -0.353 to 0.018 and were quantile divided into five groups. The FR was highest at 0.13 (Table 2) for the class -0.353 to 0.018, indicating that flooding is likely in the study areas.

Normalized difference soil index (NDSI) was used to identify signature variations in the immixing coastal swamp from satellite imagery. Deng created the normalized difference soil index/(NDSI) by reversing the adjusted normalized difference water index/ (MNDWI), which is dependent on the high reflectance of bare soil in the shortwave infrared wavelength. Despite this, the NDSI can detect large, dry bare soil parcels whereas tiny, scattered parcels are often overlooked. The thermal infrared wavelength (TIR) has been used to detect bare land [56]. The findings showed that class levels of 0.135 to 0.225 and 0.225 to 0.511 had high FR values of 0.88 and 0.183 in this

Table 3. Flood Susceptibility zone of study area under different subzones.

Zone	Class	Area (km^2)	Area %
Very low	31-44	10495	19.73
Low	44-48	10831	20.37
Moderate	48-53	10835	20.37
High	53-59	10572	19.88
Very high	59-72	10434	19.62

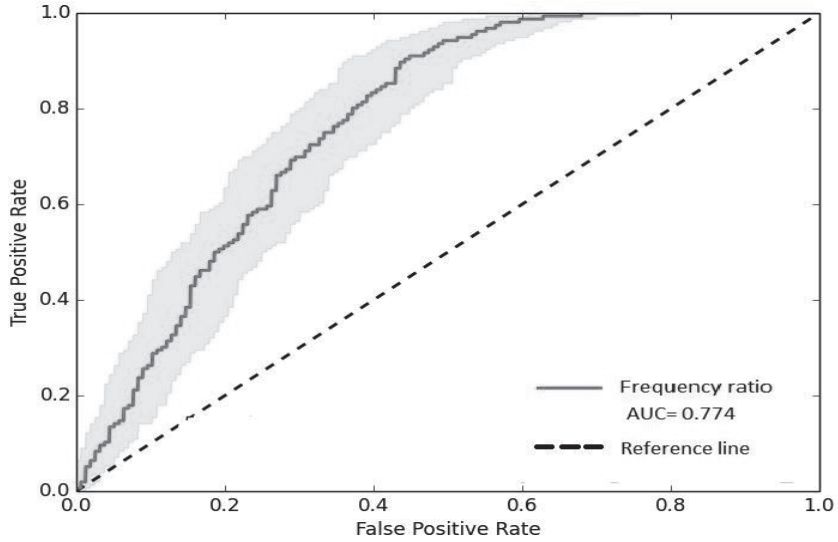

Fig 6. AUC for model performance and validation.

study area. The distance from the road is a big factor in flood susceptibility and vulnerability mapping. Flood levels are influenced significantly by impervious roads and adjacent urban surfaces. They reduce the terrain's penetration potential and double as a runoff outlet [57]. According to the results, distances from the path of less than 0.11 m and 0.11 to 0.18 m have high FR values of 8.1 and 7.2, respectively. The distance from the river is an additional factor to include when determining flood vulnerability since the places closest to the river bank are the ones that are most threatened by high water after a flood. In most cases, depth is estimated above the stream's mouth or higher than the convergence. Every land region located far away from the stream's mouth or confluence is classified as low risk, while an area located close to the stream's convergence is classified as high risk [58]. The maximum FR values in this study area are 8.18 and 1.27, respectively, with class levels between 0.45 and 0.68 and 0.68 and 1.04. The rainfall is merely a source of water in the study area, apart from glaciers. In semi-arid areas, sudden rainfall can trigger flash floods [59]. A significant number of earlier studies have found a connection between flooding and rainfall [60].In every region, the quantity of rainfall is the main significant cause of flooding. No one expects the rain to cause flooding [46]. In this study area, it is noted that the FR value (6.4) is high in areas with lots of rain (130.1 to 177.1 mm).

Land use patterns are shown as humans and natural cycles [49]. Runoff is increased in urban areas because of the extensive impervious soil, and it is increased in fallow agriculture because near is little vegetation to regulate and avoid the rapid release of water into the soil surface. Those areas are the most susceptible and vulnerable to floods and they are in danger of flooding and also soil erosion. Because of their economic wealth, housing, and high population, built-up areas along rivers are the most prone to floods [61]. In the study area, the high FR values observed in water bodies and agricultural land are 0.18 and 0.095, respectively, indicating that unprotected areas are highly susceptible and vulnerable to flooding. (Fig. 5)

(Table 3) The ratings for each subclass of all conditioning parameters are dependent on the Frequency Ratio values presented in Table 2. The vulnerable groups range from extremely high to extremely high, and they are mainly concentrated in the study area's middle (Fig. 5). Higher runoff potentiality, poor to very poorly drained soil, lower slope gradient, lower elevation, alluvial deposits, braided flood plain, and closer proximity to the main river define these high to very high flood susceptibility areas, which are significant conditioning factors for flood vulnerability and susceptibility mapping using the Frequency Ratio (FR) model. Several models are suggested and proposed by various researchers, but it is critical to assess the model's accuracy and success rate to validate it for flood susceptibility and vulnerability analysis. In terms of success rate and prediction and forecast accuracy, the FR model's performance is validated [42]. The maximum accuracy of 1.0, indicating that the model was capable of accurately predicting natural hazards without bias [62]. The accuracy prediction was calculated using the remaining 69 flood points that were not used during the model building and the success rate was calculated using 161 training flood points. Susceptibility classes ranging from 'moderate' to 'very high' are considered as possible floods that could happen in the future.

Validation through the Area under the Curve (AUC)

The flood forecast rate is determined by the prediction or forecasting curve. As a consequence, it must be evaluated as a necessary result and output

of a model to determine flood vulnerability and susceptibility mapping performance [2]. (Fig. 5) The AUC parameter was used to validate the model in this analysis, which plots factual positive rate on the y-axis against fake positive rate on the x-axis and was calculated using equation (7):

$$AUC = \frac{\sum TP + \sum TN}{P + N} \quad (7)$$

Where P represents the entire integer of floods while N represents the total integer of non-floods, and TP and TN indicate the number of pixels properly classified [63]. In the validation process, 30% of the total number of flood points were used. After review, the AUC for the model was 0.774 indicating a success rate of 0.77 percent. Despite the input data limitations and precision, this percentage was deemed satisfactory. It also describes how well the frequency ratio model and factors worked in the study area or predicted floods.

Conclusion

Flood vulnerability mapping analysis is critical for reducing destructive floods through the implementation of authentic solutions. Flood susceptibility data is a valuable tool for planners when it comes to implementing proper land use in flood-prone areas. The aim and intentions of this study are to be aware of the interconnection of flood frequency and flood factor variables in Southern Punjab and Northern Sindh, Pakistan, using a BSA-based FR model. Ten conditioning factors were taken, including slope, aspect, profile curvature, elevation, NDVI, NDSI, distance from the road, distance from the river, LULC, and rainfall, and individual layers were created with 30 m^2 resolution based on the flood inventory map. For the creation of the layers, a random sampling technique was used to pick (161) 70% of the overall flood point and (69) 30% for validation. The accuracy with which factor layers are prepared is crucial to the validation of flood-prone mapping. The final flood vulnerability map was divided into five zones: very low (19.73%), low (20.37%), moderate (20.37%), high (19.88%), and very high (19.62%) respectively. As compared to other districts such as Larkana, Rahimyar Khan, Sukkur, and Bahawalpur, Jacobabad has a high susceptible district for floods. This region is highly sensitive, and the adaptive capacity is very low. The high to the very high zone is mainly seen in the study area's middle. Higher runoff potentiality, alluvial deposits, poor to very poorly drained soil, braided food plain, lower elevation, lower slope, and proximity to the central river define these moderate to very high food susceptibility areas, which are significant conditioning factors for flood susceptibility. Susceptibility, which varies from "high" to "very high" is recognized as a possible future flood. The ROC curve was used to assess and measure the significance of the current Frequency Ratio model for vulnerability mapping. The product reveals that the approach used in this study provides consistent and correct results, with a performance rate of 77.4%. As a result, it can be accomplished that precision of the conditioning variables has a significant effect on flood susceptibility mapping since as the normal level of parameters improves, the accuracy of the model improves as well. Low slope (-2.15°-2.39°), low elevation (-68-183 m), and high NDVI (-0.353-0.018) are the most significant parameters and classes for flood-prone areas of southern Punjab and northern Sindh. There is a dire need to realize the trends of climatic extreme events especially floods and pursue the recommended adaptation strategies to manage such extremes in the future. By identifying flood-prone zones, this representation of the model will assist the government officers, planners, decision-makers, and legislatures in implementing appropriate administrative plans in the research area and limiting the development process.

Acknowledgment

This research did not receive any specific grants from funding agencies in public, commercial, or not-for-profit sectors.

Conflict of Interest

The authors declare that they have no conflict of interest.

References

1. YOUSSEF A.M., PRADHAN B., HASSAN A.M. Flash flood risk estimation along the St. Katherine road, southern Sinai, Egypt using GIS based morphometry and satellite imagery. Environmental Earth Sciences, **62** (3), 611, **2011**.
2. TEHRANY M.S., PRADHAN B., JEBUR M.N. Flood susceptibility analysis and its verification using a novel ensemble support vector machine and frequency ratio method. Stochastic Environmental Research and Risk Assessment, **29** (4), 1149, **2015**.
3. PRADHAN B. Flood susceptible mapping and risk area delineation using logistic regression, GIS and remote sensing. J Spatial Hydrol, **9**, 1, **2010**.
4. LI X., ZHANG Q., SHAO M., LI Y. A comparison of parameter estimation for distributed hydrological modelling using automatic and manual methods. Advanced Materials Research, 356–360, 2372–2375, **2012**.
5. WANG Y., HONG H., CHEN W., LI, S., PAMUČAR D., GIGOVIĆ L., DROBNJAK S., BUI D.T., DUAN H. A hybrid GIS multi-criteria decision-making method for flood susceptibility mapping at Shangyou, China. Remote Sensing, **11** (1), **2019**.

6. CLOKE H.L., PAPPENBERGER F. Ensemble flood forecasting: A review. Journal of Hydrology, **375** (3-4), 613, **2009**.
7. BRONSTERT A. Floods and climate change: Interactions and impacts. Risk Analysis, **23** (3), 545, **2003**.
8. WHO. Disaster data-key trends and statistics in world disasters report. WHO, Geneva, Switzerland. **2003**.
9. OPOLOT E. Application of remote sensing and geographical information systems in flood management: a review. Research journal of applied sciences engineering and technology, **6** (10), 1884, **2013**.
10. GUHA-SAPIR D., SANTOS I., GUHA-SAPIR D., HOYOIS P. The Frequency and Impact of Natural Disasters Oxford Scholarship Online The Frequency and Impact of Natural Disasters. May **2016**, 1, **2013**.
11. HARAGUCHI M., LALL U. Flood risks and impacts: a case study of Thailand's floods in 2011 and research questions for supply chain decision making. Int J Disaster Risk Reduct. **14**, 256, **2015**.
12. DHAR O.N., NANDARGI S. Hydrometeorological Aspects of Floods in India. **1994**, 1, **2003**.
13. DE GROEVE T., KUGLER Z., BRAKENRIDGE G.R. Near real time flood alerting for the global disaster alert and coordination system. Intelligent Human Computer Systems for Crisis Response and Management, ISCRAM 2007 Academic Proceedings Papers, 33-39, **2007**.
14. AHMAD D., AFZAL M. Flood hazards and factors influencing household flood perception and mitigation strategies in Pakistan. Environmental Science Pollution, **27**, 1, **2020**.
15. NDMA. Annual Report, **148**, 148, **2017**.
16. ALEXANDER M., PRIEST S., MEES H. A framework for evaluating flood risk governance. Environmental Science and Policy, **64**, 38, **2016**.
17. KHAN A., KHAN B., QASIM S., KHAN S. Causes, Effects and Remedies: A Case Study of Rural Flooding in District Charsadda, Pakistan. Journal of Managerial, January. **2013**.
18. SORIANO I.R.S., PROT J.C., MATIAS D.M. Expression of tolerance for Meloidogyne graminicola in rice cultivars as affected by soil type and flooding. Journal of Nematology, **32** (3), 309, **2000**.
19. HAQ M., AKHTAR M., MUHAMMAD S., PARAS S., RAHMATULLAH J. Techniques of Remote Sensing and GIS for flood monitoring and damage assessment: A case study of Sindh province, Pakistan. Egyptian Journal of Remote Sensing and Space Science, **15** (2), 135, **2012**.
20. ESTEVES L.S. Consequences to flood management of using different probability distributions to estimate extreme rainfall. Journal of Environmental Management, **115**, 98, **2013**.
21. SINDH POPULATION POLICY. Population Welfare Department Government of Sindh. **2016**.
22. WAQAS H., LU L., TARIQ A., LI Q., BAQA M.F., XING J., SAJJAD A. Flash flood susceptibility assessment and zonation using an integrating analytic hierarchy process and frequency ratio model for the chitral district, khyber pakhtunkhwa, pakistan. Water (Switzerland), **13** (12), **2021**.
23. OUMA Y.O., TATEISHI R. Urban flood vulnerability and risk mapping using integrated multi-parametric AHP and GIS: Methodological overview and case study assessment. Water (Switzerland), **6** (6), 1515, **2014**.
24. LIAO X., CARIN L. Migratory logistic regression for learning concept drift between two data sets with application to UXO sensing. IEEE Transactions on Geoscience and Remote Sensing, **47** (5), 1454, **2009**.
25. DEWAN T.H. Societal impacts and vulnerability to floods in Bangladesh and Nepal. Weather and Climate Extremes, **7**, 36, **2015**.
26. PAPAIOANNOU G., VASILIADES L., LOUKAS A. Multi-criteria analysis framework for potential flood prone areas mapping. Water ResourManag, **29** (2), 399, **2015**.
27. RAHMATI O., ZEINIVAND H., BESHARAT M. Flood hazard zoning in Yasooj region, Iran, using GIS and multi-criteria decision analysis. Geomatics, Natural Hazards and Risk, **7** (3), 1000, 2016, **2016**.
28. POUSSIN J.K., BOTZEN W.J.W., AERTS J.C.J.H. Factors of influence on flood damage mitigation behavior by households. Environ Sci Policy **40**, 69, **2014**.
29. KONADU D.D., FOSU C. Digital Elevation Models and GIS for watershed modelling and flood prediction – A case study of Accra Ghana. Appropriate Technologies for Environmental Protection in the Developing World – Selected Papers from ERTEP 2007, 325, **2009**.
30. MERZ B., THIEKEN A.H., GOCHT M. Flood risk mapping at the local scale: concepts and challenges. In: Begum S, Stive MJF, Hall JW (eds) Flood risk management in Europe. Advances in Natural and Technological Hazards Research, **25**, 231, **2007**.
31. PRADHAN B. Flood susceptible mapping and risk area delineation using logistic regression. GIS and remote sensing. J Spatial Hydrol, **9**, 1, **2010**.
32. OHLMACHER G.C., DAVIS J.C. Using multiple logistic regression and GIS technology to predict landslide hazard in northeast Kansas, USA. EngGeol **69**, 331, **2003**.
33. KIA M.B., PIRASTEH S., PRADHAN B., MAHMUD A.R., SULAIMAN W.N.A., MORADI A. An artificial neural network model for flood simulation using GIS: Johor River Basin, Malaysia. Environmental Earth Sciences, **67** (1), 251, **2012**.
34. BATES P.D., MARKS K.J., HORRITT M.S. Optimal use of high-resolution topographic data in flood inundation models. Hydrological Processes, **17** (3), 537, **2003**.
35. PARDHAN B., SHAFEE M., PIRASTEH M. Maximum flood prone area mapping using RADARSET images and GIS: Kelantan River Basin. International Journal Geoinformation **5** (2), 49, **2009**.
36. REGMI A.D., DEVKOTA K.C., YOSHIDA K., PRADHAN B., POURGHASEMI H.R., KUMAMOTO T., AKGUN A. Application of frequency ratio, statistical index, and weights-of-evidence models and their comparison in landslide susceptibility mapping in Central Nepal Himalaya. Arab J Geoscience, **7** (2), 725, **2013**.
37. YALCIN A. GIS-based landslide susceptibility mapping using analytical hierarchy process and bivariate statistics in Ardesen (Turkey): Comparisons of results and confirmations. Catena, **72** (1), 1, **2008**.
38. LEE M., KANG J., JEON S. Application of frequency ratio model and validation for predictive Korea Adaptation Center for Climate Change , Korea Environment Institute, 613-2 Bulgwang-Dong. Geoscience and Remote Sensing Symposium (IGARSS), IEEE International. IEEE, **1**, 895, **2012**.
39. JEBUR M.N., PRADHAN B., TEHRANY M.S. Optimization of landslide conditioning factors using very high-resolution airborne laser scanning (LiDAR) data at catchment scale. Remote Sens Environ, **152**, 150, **2014**.

40. AKGUN A., DAG S., BULUT F. Landslide susceptibility mapping for a landslide-prone area (Findikli, NE of Turkey) by likelihood-frequency ratio and weighted linear combination models. Environmental Geology, **54** (6), 1127, **2008**.
41. PHAM B.T., AVAND M., JANIZADEH S., PHONG T.V., AL-ANSARI N., HO L.S., DAS S., LE H.V., AMINI A., BOZCHALOEI S.K., JAFARI F. GIS based hybrid computational approaches for flash flood susceptibility assessment. Water, **12** (3), 683, **2020**.
42. CHUNG C.J.F., FABBRI A.G. Validation of spatial prediction models for landslide hazard mapping. Natural Hazards, **30** (3), 451, **2003**.
43. POURGHASEMI HR., PRADHAN B., GOKCEOGLU C. Application of fuzzy logic and analytical hierarchy process (AHP) to landslide susceptibility mapping at Haraz watershed, Iran. Natural Hazards, **63** (2), 965, **2012**.
44. TIEN BUI D., PRADHAN B., LOFMAN O., REVHAUG, I. Landslide susceptibility assessment in vietnam using support vector machines, decision tree, and nave bayes models. Mathematical Problems in Engineering, **2012a**.
45. TIEN BUI,D., PRADHAN B., LOFMAN O., REVHAUG I., DICK O.B. Spatial prediction of landslide hazards in Hoa Binh province (Vietnam): A comparative assessment of the efficacy of evidential belief functions and fuzzy logic models. Catena, **96**, 28, **2012b**.
46. SAHANA M., PATEL P.P. A comparison of frequency ratio and fuzzy logic models for flood susceptibility assessment of the lower Kosi River Basin in India. Environmental Earth Sciences, **78** (10), 1, **2019**.
47. DAS S. Geospatial mapping of flood susceptibility and hydro-geomorphic response to the floods in Ulhas basin, India. Remote Sensing Applications: Society and Environment, **14** (February), 60, **2019**.
48. KHOSRAVI K., MELESSE A.M., SHAHABI H., SHIRZADI A., CHAPI K., HONG H. Flood susceptibility mapping at Ningdu catchment, China using bivariate and data mining techniques. Extrem Hydrol Clim Var, 419, **2019**.
49. KHOSRAVI K., NOHANI E., MAROUFINIA E., POURGHASEMI H.R. A GIS-based flood susceptibility assessment and its mapping in Iran: a comparison between frequency ratio and weights-of-evidence bivariate statistical models with multi-criteria decision-making technique. Natural Hazards, **83** (2), 947, **2016**.
50. RADMEHR A., ARAGHINEJAD S. Flood Vulnerability Analysis by Fuzzy Spatial Multi Criteria Decision Making. Water Resources Management, **29** (12), 4427, **2015**.
51. SHAFIZADEH-MOGHADAM H., VALAVI R., SHAHABI H., CHAPI K., SHIRZADI A. Novel forecasting approaches using combination of machine learning and statistical models for flood susceptibility mapping. Journal of Environmental Management, **217**, 1, **2018**.
52. ERCANOGLU M., GOKCEOGLU C. Assessment of landslide susceptibility for a landslide prone area (north of Yenice, NW Turkey) by fuzzy approach. Environ Geol. **41**, 20, **2002**.
53. SIDLE R.C., OCHIAI H. Landslides: processes, prediction, and landuse. American Geophysical Union, Washington, D.C. Water Res Monograph, **18**, 312, **2006**.
54. RAZANDI Y., POURGHASEMI H.R., NEISANI N.S., RAHMATI O. Application of analytical hierarchy process, frequency ratio, and certainty factor models for groundwater potential mapping using GIS. Earth Science Informatics, **8** (4), 867, **2015**.
55. PAUL G.C., SAHA S., HEMBRAM T.K. Application of the GIS-Based Probabilistic Models for Mapping the Flood Susceptibility in Bansloi Sub-basin of Ganga-Bhagirathi River and Their Comparison. Remote Sensing in Earth Systems Sciences, **2** (2-3), 120, **2019**.
56. AGHDAM I.N., VARZANDEH M.H.M., PRADHAN B. Landslide susceptibility mapping using an ensemble statistical index (Wi) and adaptive neuro-fuzzy inference system (ANFIS) model at Alborz Mountains (Iran). Environ Earth Sci. **75**, 1, **2016**.
57. SHUSTER W.D., BONTA J., THURSTON H., WARNEMUENDE E., SMITH D.R. Impacts of impervious surface on watershed hydrology: A review. Urban Water Journal, **2** (4), 263, **2005**.
58. CHAPI K., SINGH V.P., SHIRZADI A., SHAHABI H., BUI D.T., PHAM B.T., KHOSRAVI K. A novel hybrid artificial intelligence approach for flood susceptibility assessment. Environmental Modelling and Software, **95**, 229, **2017**.
59. DAS S. Geographic information system and AHP-based flood hazard zonation of Vaitarna basin, Maharashtra, India. Arabian Journal of Geosciences, **11** (19), **2018**.
60. HONG H., PANAHI M., SHIRZADI A., MA T., LIU J., ZHU A.X., CHEN W., KOUGIAS I., KAZAKIS N. Flood susceptibility assessment in Hengfeng area coupling adaptive neuro-fuzzy inference system with genetic algorithm and differential evolution. Science of the Total Environment, **621**, 1124, **2018**.
61. NANDI A., MANDAL A., WILSON M., SMITH D. Flood hazard mapping in Jamaica using principal component analysis and logistic regression. Environmental Earth Sciences, **75** (6), 1, **2016**.
62. PRADHAN B., BUCHROITHNER M.F. Comparison and validation of landslide susceptibility maps using an artificial neural network model for three test areas in Malaysia. Environ Eng Geosci, **16**, 107, **2010**.
63. TIEN BUI D. New hybrids of anfis with several optimization algorithams for flood susceptibility modeling. Water, **10** (9), 1210, **2018**.